Resolving Single Cone Inputs to Visual Receptive Fields

Lawrence C. Sincich*, Yuhua Zhang, Pavan Tiruveedhula,
Jonathan C. Horton and Austin Roorda

* Corresponding author address:
Beckman Vision Center, University of California, San Francisco, San Francisco, CA 94143
(email: sincichl@vision.ucsf.edu)

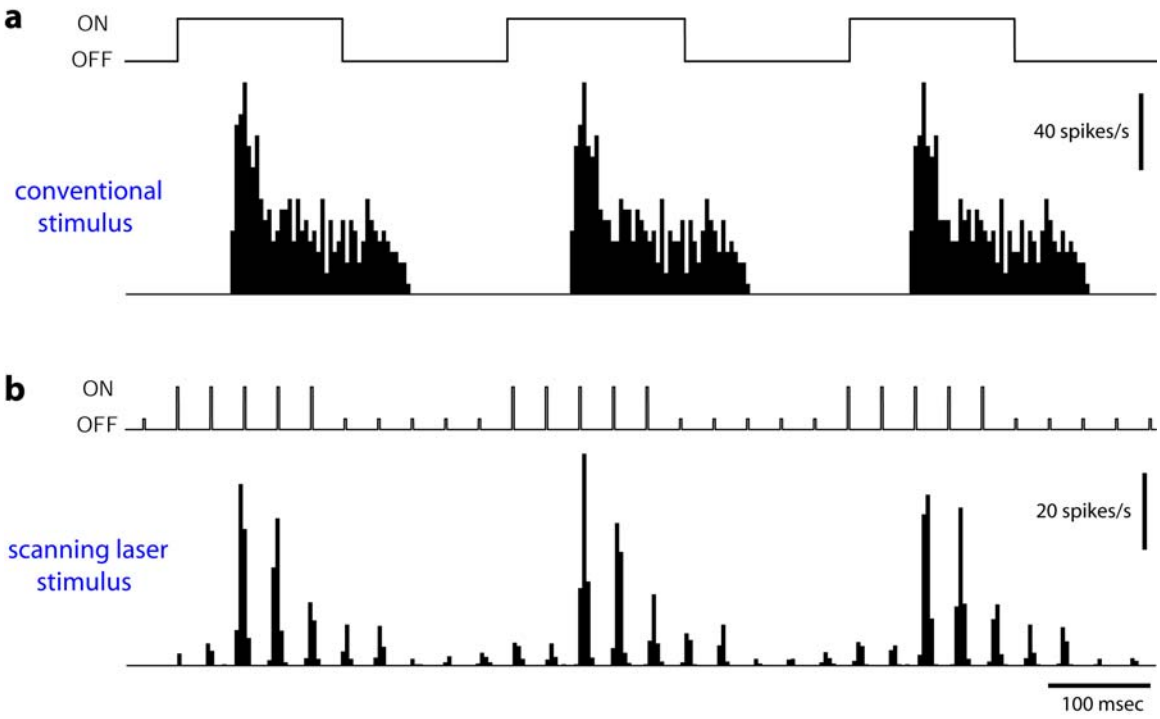

Supplementary Figure 1. Comparison of parvocellular LGN neural responses to continuous and 30 Hz raster scanned stimuli. (**a**) Spike histogram recorded with an LED stimulus flashing at 3 Hz in the receptive field center. After a mean latency of 51 ms, the neuron showed a transient ON response which then decreased during the remainder of the ON phase of the stimulus. This adapting response profile is typical for parvocellular LGN neurons in the macaque[1]. (**b**) A different ON-center parvocellular cell (Neuron 1 in the main text) recorded with the AOSLO during a 3 Hz flashing stimulus modulated at a 30 Hz frame rate. The latency of the response is similar to that seen with the conventional stimulus shown in **a**. There is a 0.4% light leak through the AOM which controls stimulus switching, and this leads to a small pulse during the OFF phase of the stimulus as the raster scans past the receptive field. The envelope of the spike histogram produced with a scanning laser resembles the histogram generated with the conventional stimulus. The spike histogram during the first stimulus cycle represents the data in the middle panel of Fig. 1b in the main text, collapsed along the spatial dimension. All histograms are complied from multiple stimulus repetitions.

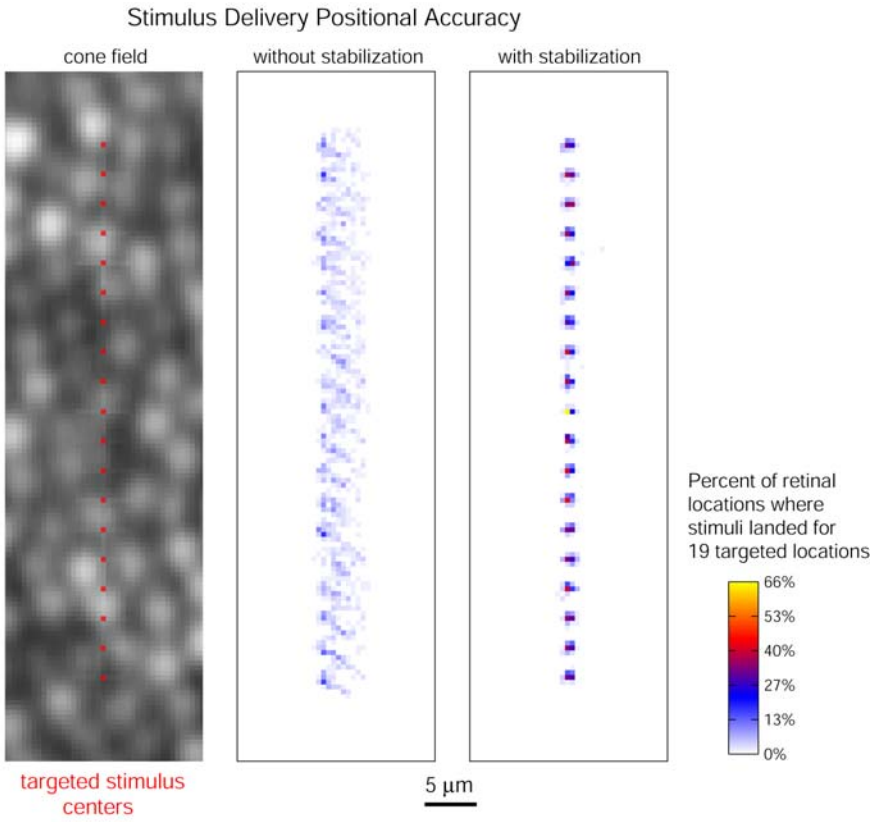

Supplementary Figure 2. Stimulus delivery depends on stabilization of targeted retinal positions. For the 19 retinal locations specified for Neuron 1 (left, **Fig. 1b**), the stimulus center positions are plotted without stabilization (middle), reflecting the cardiac-induced motion of the retina. With stabilization turned on (right), this motion artifact is nearly eliminated, with >95% of the stimulus centers landing within 1 pixel (0.476 µm) of the intended retinal locations.

Supplementary Methods

Extracellular recording procedures

Experiments were conducted on two adult male *Macaca mulatta*, using procedures approved by the UCSF Institutional Animal Care and Use Committee, in accordance with NIH guidelines, and are based on published methods[2]. Anesthesia was induced with ketamine HCl (10 mg/kg, i.m.). The animal was intubated endotrachially and anesthesia maintained with 1.5% isoflurane in a 1:1 mixture of N_2O:O_2 using artificial respiration. We monitored electro-cardiogram signals (waveform and heart rate), respiratory rate, body temperature, blood oxygenation (S_pO_2), endtidal CO_2, urine output, and inspired/expired levels of anesthetic gases throughout the experiment. A 5% dextrose in 0.45% saline solution was given intravenously at ~3 ml/kg/hr. The animal was placed in a stereotaxic frame, which itself was mounted on a gimbal with the center of motion positioned at the pupil of the eye to be imaged. The gimbal enabled us to rotate the eye at will, to image different retinal locations (within ±16° horizontally and ±10° vertically), which is required because the optical axis of the adaptive optics scanning laser ophthalmoscope (AOSLO) system is fixed. We made a craniotomy at a location suitable for dorsal access to the LGN (7-17 mm mediolaterally, 2-12 mm anterior-posteriorly). Prior to recording, we established neuromuscular blockade with vecuronium bromide (60 μg/kg/hr) to minimize eye movements. Pupils were dilated with 1% cyclopentolate hydrochloride (Cyclogyl, Alcon Laboratories), and we installed contact lenses to protect the corneas. Clarity of the optics were checked regularly and adjusted throughout the course of each experiment.

For extracellular recording, we used a single Epoxylite-coated tungsten electrode (5-8 MΩ, FHC Inc.) lowered through a stainless steel guide tube positioned 5 mm above the LGN. Differential amplification of the cellular potentials was done in two stages, using a 10× headstage amplifier followed by 100× amplification (Model 1800, A-M Systems). Analog potentials were bandpass filtered between 0.3-3 kHz before being passed to a digital data acquisition system sampling at 25 kHz (Power 1401, Cambridge Electronic Design). Along each electrode penetration, the neurons were alternately driven by contra- and ipsilateral eyes, depending on LGN lamina[3]. We kept track of these transitions to determine whether parvocellular or magnocellular neurons were being recorded.

Visual stimulus delivery

Details of the optical system design for the AOSLO have been published elsewhere[4]. We describe pertinent features of the system briefly here. Mirrors were used through the optical path to keep the system compact (75 × 75 cm footprint) and to avoid chromatic aberrations. Wave aberrations were measured over a 6 mm pupil and corrected in closed-loop with a 3.5 μm stroke MEMS (micro-electro-mechanical system) deformable mirror (Boston Micromachines Corp). In the AOSLO, aberrations are corrected on the way into the eye to produce a focused spot on the retina and on the way out of the eye to refocus the light from the retina through the confocal pinhole.

Continuously acquired 512 × 512 pixel confocal images of light reflecting off the retina were generated at a 30 Hz frame rate using a near-infrared 840 nm low coherent super-luminescent diode source (Superlum, Russia). Without AO correction, cones near the fovea were not resolvable. Image streams from this wavelength channel were also used to record retinal motion and calculate the location for stimulus placement.

For stimulus delivery, a high frequency acousto-optic modulator (AOM; Brimrose Corporation, Mass.) was used in the path of a second scanning light source (680 nm wavelength) to generate patterned stimuli on the retina[5]. The modulation was synchronized with the horizontal line of the raster scan, whose frequency was governed by the 16 kHz resonant scanning mirror. Upon each horizontal mirror return, a digital-to-analog (DA) waveform generator produced a stream of analog voltages corresponding to a single line of the raster scan. These voltages drove the AOM, which in turn modulated the scanning laser's intensity. The extinction ratio of the AOM between the 'on' and 'off' settings was 0.4%, so with a typical stimulus luminance of 100 cd/m^2, the background field of the raster scan was supplemented with a uniform luminance of about 0.4 cd/m^2. The total background luminance during operation was ~2.4 cd/m^2 (imaging and stimulus lasers combined), which was more than enough to elicit steady neural responses at the frame rate (see Supplementary Fig. 1 and Figs. 1b, 2). This background was bright enough to saturate any rod photoreceptors, and therefore they were unlikely to contribute to the neural responses. The background activity also had the advantage that inhibitory responses could be recorded, when they were present.

Because the frame rate was 30 Hz, well within the temporal frequency range of many LGN neurons[6], the responses were characteristically phase-locked at 30 Hz. Responses to stimuli flashing at lower frequencies (typically 3 Hz) therefore appeared as a 30 Hz pattern modulated by the envelope of the stimulus (Supplementary Fig. 1). Despite this artifact, both ON and OFF responses could be recorded in respective cell types, as well as appropriate inhibitory responses during the non-preferred phase of each stimulus.

Stimulus images were loaded into a queue on the DA board so that complex stimulus patterns could be projected directly onto the retina. The stimulus light was provided by a low-coherent 680 nm wavelength super-luminescent diode. The different wavelengths used for imaging and stimulation required that transverse and longitudinal chromatic aberrations (TCA and LCA) be corrected to bring the two lasers into alignment at the retina, as such aberrations would otherwise leave the scanned paths out of register[7]. LCA was corrected by precorrecting the focus of the red source relative to the IR source prior to entering the eye. Videos from a second confocal imaging channel for the 680 nm light were viewed alongside the IR video to ensure that both lasers were focused in the same retinal plane. To determine TCA, we aligned the 680 nm source and its detector to minimize the lateral shifts in retinal videos where we temporally alternated the source between 680 nm and 840 nm. The alternating TCA videos were analyzed off-line to compute any remaining shifts. LCA was constant, but unique TCA adjustments and corrections were necessary at each cone field recording site.

In anesthetized macaques under neuromuscular blockade, there is eye motion due to cardiac pulsations (see Supplementary Video 1). This motion can induce periodic retinal movements of 10 μm or more, several times the width of a cone[8]. To deliver stimuli repeatedly to the same location in the retina, we used a video-based algorithm to track retinal motion at 1 kHz. These motion signals were used to predict and deliver stimuli with a 5 msec lag time[9]. By minimizing the lag between prediction and delivery, the precision of the delivered stimulus (standard deviation of position) was 0.06 arcmin, or about one tenth the diameter of the smallest cones in the retina[10]. A video of the stabilized stimulus delivery for the cone mapping shown in Fig. 1b is provided (Supplementary video 2). The realized stimulus delivery locations for this cell showed a spread of ±1 pixel in stabilized mode (Supplementary Fig. 2) . Because the stimulus light follows the same AO corrected path as the imaging light, the stimulus is delivered

with ultra-sharp precision. Most of the energy in an AO-corrected spot is likely to fall within a single cone photoreceptor[11].

The stimulus size and geometry were selectable from predefined files. Duty cycle and flash frequency were independently set, within integer limits of the 30 Hz frame rate. Stimulus position was selected manually at one point within a retinal image of 512 × 512 pixels (1.2° × 1.2°), specifying either a row or a column positions centered on that location. When the stimulus sequence was started, stimuli were flashed in pseudorandom order an equal number of times at each specified position. For each stimulus run, a video was saved, containing the 840 nm images along with stimulus position and state coded as a small fiducial cross into each frame (white = on, black = off). Memory capacity limited each video to ~2 minutes. Depending on the specified stimulus, each stored video contained multiple repeats of a stimulus sequence, and at least 5 videos of each condition were recorded.

Prior to use, the power levels of both lasers were calibrated to ensure that exposure levels remained well below the safety thresholds established by the American National Standards Institute (ANSI Z136.1-2000, Orlando: Laser Institute of America, 2000).

Data analysis

Each physiological experiment included a continuous digital record of microelectrode voltage coordinated with stimulus onset, frame synchronization, and diagnostic vital signs. Single LGN neurons were identified by conventional spike sorting. In conjunction with the stimulus movies, we constructed 2-dimensional spike density histograms. Each stimulus location was represented by a row in the histogram containing the spike response plotted in time (Figs. 1b, 2). The space-time histograms show the temporal variation in the response, which can include information regarding cone type because the graded cone response generates threshold activity in ganglion cells at different latencies for different wavelengths or intensities. For instance, a 680 nm stimulus of a given intensity will more slowly activate an M cone pathway than an L cone pathway. Spike probability for each stimulus flash was computed as the likelihood of one or more spikes per trial for the time period indicated in each figure.

To estimate the spatial extent of the light energy distribution as delivered over the course of all stimulus trials, we computed the point-spread function (PSF) of a stimulus pixel as diffraction-limited for a 6 mm pupil with 680 nm wavelength light. For each location, the PSF was then convolved with the stimulus geometry and the stimulus location density function after stabilization for all stimulus trials (for an example, see one of the density plots for a single location in Supplementary Fig. 2). For the stimulus geometries we used, ~66% of the energy distribution fell within the bounds of the stimuli indicated in Figures 1 and 2.

Supplementary References

1. Schiller, P.H. & Malpeli, J.G. Functional specificity of lateral geniculate nucleus laminae of the rhesus monkey. *J Neurophysiol* **41**, 788-797 (1978).
2. Sincich, L.C., Adams, D.L., Economides, J.R. & Horton, J.C. Transmission of spike trains at the retinogeniculate synapse. *J Neurosci* **27**, 2683-2692 (2007).
3. Malpeli, J.G., Lee, D. & Baker, F.H. Laminar and retinotopic organization of the macaque lateral geniculate nucleus: magnocellular and parvocellular magnification functions. *J Comp Neurol* **375**, 363-377 (1996).
4. Zhang, Y., Poonja, S. & Roorda, A. MEMS-based adaptive optics scanning laser ophthalmoscopy. *Opt Lett* **31**, 1268-1270 (2006).
5. Poonja, S., Patel, S., Henry, L. & Roorda, A. Dynamic visual stimulus presentation in an adaptive optics scanning laser ophthalmoscope. *J Refract Surg* **21**, S575-580 (2005).
6. Derrington, A.M. & Lennie, P. Spatial and temporal contrast sensitivities of neurones in lateral geniculate nucleus of macaque. *J Physiol* **357**, 219-240 (1984).
7. Grieve, K., Tiruveedhula, P., Zhang, Y. & Roorda, A. Multi-wavelength imaging with the adaptive optics scanning laser ophthalmoscope. *Optics Express* **14**, 12230-12242 (2006).
8. Forte, J., Peirce, J.W., Kraft, J.M., Krauskopf, J. & Lennie, P. Residual eye-movements in macaque and their effects on visual responses of neurons. *Vis Neurosci* **19**, 31-38 (2002).
9. Arathorn, D.W., *et al.* Retinally stabilized cone-targeted stimulus delivery. *Optics Express* **15**, 13731-13744 (2007).
10. Roorda, A., *et al.* Real-time correction of eye movement distortions in adaptive optics scanning laser ophthalmoscope images. in *Invest Ophthalmology and Visual Science* (2007).
11. Hofer, H., Singer, B. & Williams, D.R. Different sensations from cones with the same photopigment. *J Vis* **5**, 444-454 (2005).